JOURNAL OF MATERIALS SCIENCE **39** (2004) 207–214

Structural differences in the cortical bone of Turkey tibia

YU-SHUIUAN CHEN, C. RAMACHANDRA, S. N. TEWARI*
Department of Chemical Engineering, Cleveland State University, Cleveland, OH 44115, USA
E-mail: s.tewari@csuohio.edu

Different regions namely anterior, posterior, medial and lateral, of the cortical bone in six sections in the diaphysis from proximal to the distal end of a Turkey tibia were evaluated for structural differences. The predominant feature, Haversian canals showed high area fraction (can be viewed as high porosity) in the posterior region as compared to the anterior region and this difference is attributed to the high compressive and tensile stress states in the respective regions. With increasing size, the Haversian canals deviated from circular shapes in cross section. The distance from the lacunae to the center of the Haversian canal showed an increase with the size of the canals. However, the canal to lacunae-canal distance ratio is independent of the anterior and posterior regions. It was found that majority of the lacunae are placed at a distance of about 2.5 to 3 times the Haversian canal radius. At the ultrastructural level, periodic banding of the collagen fibers showed a bimodal banding in the anterior region while only one finer banding distribution in the posterior region and could probably the result of the different stress states in the two regions. The Haversian canals in the three dimensional reconstruction showed branching, twisted canals and Haversian space and resemble Cohen and Harris model. Differences in stress in different regions cause structural changes in bone.

1. Introduction

There have been studies regarding ultrastructural and molecular features of bone in different species with some general agreements and also differences. Haversian systems are a prominent feature in cortical bone. Studies on Haversian systems have predominantly focused on the physiological aspects where the histomorphometric analysis and the cortical remodeling cycle are among the central topics. Amprino and Bairati [1] studied the Haversian systems in cross sections of human and animal long bones and described the changes in shape, size, and regularity of the Haversian systems in single cross sections. Brockstedt *et al.* [2] quantified the influence of age and sex on the Haversian systems/cortical bone mass in normal human iliac crest bone biopsies with various measurements, including the cortical porosity and the diameters of the osteons, the Haversian canals, and the remodeling space. However, the Haversian systems have not been thoroughly characterized in terms of the distributions in different regions of the cortical bone.

Associated with the Haversian systems are the lacunae, the small chambers in the loose lamellae where an osteocyte, shaped like a plum stone, is located. It has been shown by Ardizzoni [3] that the size of these lacunae decreases from the outer region of the osteons towards its interior, in association with a similar decrease in the loose-lamellae thickness. However, this study did not take into account the location of the osteons. Further, there is no study in the literature regarding the distribution of the distance between the Haversian canal and the lacunae within the same Haversian system.

While there are still many aspects of the Haversian systems and the associated lacunae that are to be understood, currently the finer aspects of the structure are studied with the relatively new tool namely, the Atomic Force Microscope (AFM). A few studies have been reported. Nicolella *et al.* [4] applied the AFM to characterize the damaged cortical bone and described the surface preparation techniques involved. Baranauskas, Garavello-Freitas, and Jingguo [3] used AFM to study the reconstruction of the injured bone by comparing with the intact bone structure of rat tibia. The latest research conducted by Sasaki *et al.* [5] found thread-like objects with periodic patterns comparable to the collagen D-period of the Hodge-Petruska model, indicating that the threads are collagen fibrils. However, no study has been noted to compare the finer structure of different regions of the same bone.

Mechanical and biological characteristics of bone are expected to depend upon the three dimensional structure of the Haversian system. Cohen and Harris [6] used serial sectioning to reconstruct the osteons network in a dog femur. He simulated the osteons path by

*Author to whom all correspondence should be addressed.

color-coded wires, and reported that the osteons run in long clockwise spirals from the periosteal to the endosteal surface of the bone. Hĕrt *et al.* [7] thoroughly examined the orientations of osteons in the long bone of a man and suggested that osteons exist in two helical systems running in opposite directions, and lying on the opposite sides of the diaphysis. This research was based on observations on several longitudinal sections of the bone, and not on the three-dimensional reconstruction using serial sections. Stout *et al.* [8] used serial sectioning to create three-dimensional reconstrction of the Haversian systems and did not see such spiraling. However, they also did not use any reference to properly align images from their various sections. In order to create an accurate three-dimensional representation based on serial sections it is crucial that a suitable reference be used to precisely align the transverse images. We are not aware of any such study.

In view of the above differences, the present study is aimed to understand the characteristics of the Haversian system, and the changes due to the loading environment in the turkey tibia which would eventually help in modeling for implants. The turkey tibia should help in understanding the human bone ultimately.

2. Experimental procedures

The cartilage, ligaments and the epiphysis were removed from the left tibia of a turkey of unknown age, weighing about 6.3 kg. The central part of the bone was fixed in 70% ethyl alcohol for 2 days. Slow speed diamond saw was used to cut six transverse sections (0.5 to 1.0 cm thick) 1, 2, 3, 4, 5 and 6 (shown in Fig. 1a) along the longitudinal direction from the proximal to the distal end of the diaphysis (central shaft of a long bone) of the tibia. These were washed in running tap water, alcohol dehydrated, air dried at room temperature, and mounted in epoxy resin.

Transverse section surfaces for optical microscopy examination were polished using silicon carbide abrasive paper of decreasing grit size (400, 600, and 800 grit) under running tap water. The final polishing was carried out on the VIBROMET (Buehler Ltd.) with a 0.5 μm alumina powder suspension for about 20–30 min and cleaned ultrasonically. For examination in AFM, the specimens prepared in the manner for optical microscopy were decalcified by immersing in a 30% phosphoric acid solution for 5 min, cleaned with distilled water in an ultrasonic bath, and air dried at room temperature in order to remove the smeared layer [4] and thus help in revealing the ultra-structural details.

The HL Image software was employed to capture images (50× magnification) to cover different regions (Fig. 1b) of the polished surface of each section using Nikon optical microscope. Montages were created by joining the individual images by using SigmaScan Pro 4 (Jandel Scientific).

Fig. 2 is a typical optical microphotograph of the transverse section showing the features, Haversian canals and lacunae. The Haversian canal boundaries were identified using the Sigmascan Pro software. The software was used to measure the cross sectional area, perimeter, shape factor, and the coordinates of the geometric center of the Haversian canals. A software SigmaStat (v. 2.03, SPSS Inc.) was used to analyze the data for their means, standard deviations, and values of skewness, and to carry out the normality test, analysis of variance (ANOVA), and multiple comparisons. Another software, SigmaPlot (v. 4.0, SPSS Inc.) was used to create the histograms, box plots, and side-by-side confidence interval plots.

Shape Factor (SF) is an indication of how circular an object is. It is calculated as SF $= 4\pi$ Area/Perimeter. A perfect circle has a shape factor of 1, and a line has shape factor approaching zero.

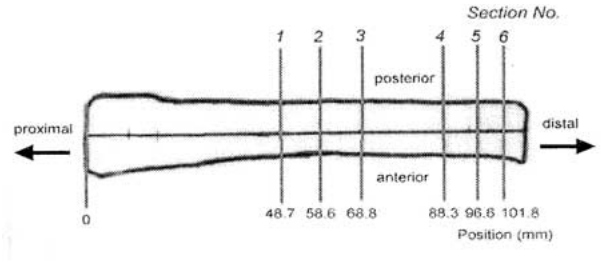

(a)

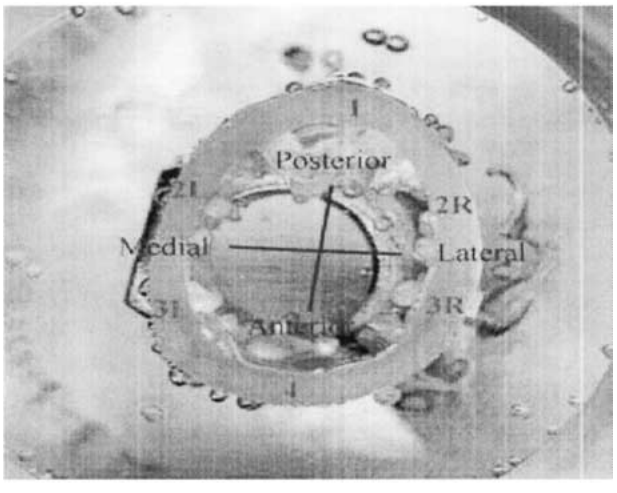

(b)

Figure 1 (a) Schematic showing the transverse sections of the turkey tibia. (b) Regions are shown on the actual transverse bone cross section (Anterior to Posterior to outside edges is about 16 mm).

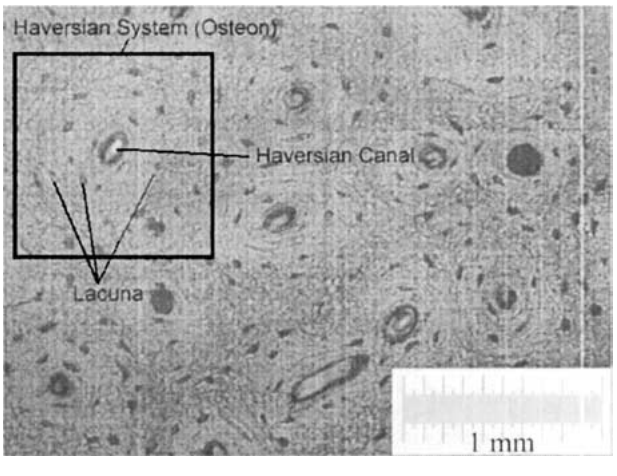

Figure 2 Dried ground cross section through Haversian systems of turkey tibia. Bar = 1 mm.

A minimum spanning tree (MST) is a connected graph without any close loop, which contains all the geometric centers of the Haversian canals and for which the sum of the edge weights is minimal. Such a tree represents the shortest total length of branches in order to connect all the Haversian canals. We have used Prim's algorithm [9] where an arbitrary center of canal is chosen initially as the tree root. The center of canal nearest to the tree is identified and is joined to the tree. This process is repeated until all the points are connected to this minimum spanning tree. The branch length distribution represents the nearest neighbor distribution of the Haversian canals.

The distances between the center of the Haversian canal and its surrounding lacunae in the same Haversian system were measured using SigmaScan. These distances are defined as the lacunae-canal distances. The data were analyzed by the statistics software, SAS (SAS Institute, Cary, NC).

A serial sectioning and three dimensional reconstruction technique described in [10] was used in this study. Reference holes about 200 μm in diameter and 0.15 cm long are drilled into the sample that is mounted in epoxy. These holes, filled by epoxy, are later on used as reference during recording of the transverse images. A Leica ultramiller equipped with a microscope and in-situ image recording facility was used for serial sectioning with 2 to 3 μm step. Three-dimensional images of the Haversian canals were reconstructed from twenty-five cross-sectional optical images (200×) using the SurfDriver software. This technique may not allow one to follow the Haversian canals over long distances, but it does yield a highly accurate three-dimensional representation [10].

3. Results

The results are presented under four different sections namely, (1) the characterization of Haversian canals, (2) analyses of the lacunae-canal distance distributions, (3) the atomic force microscopy of features associated with collagen fibers and (4) the three-dimensional reconstruction of the Haversian canals.

3.1. Haversian canal characterization

The data of Haversian canals were collected from six different *regions* in one section, and there are six *sections* along the longitudinal direction of the central shaft from the proximal to the distal end of the tibia. The six *regions* and the six *sections* are defined in Fig. 1a and b. It has to be stressed that any two corresponding regions from any adjacent sections do not occupy the same area and may not be exactly on top of each other. Due to plane sectioning effect, the Haversian canals appear irregular and asymmetrical. Further, there could be some interference from the Volkmann's canals.

There are four measurements in this Haversian canal characterization; the Cross Sectional Area of the canal (CA), Shape Factor (SF), Mean Branch Distance from the MST (MST), and Area Fraction of the observed region. Shape Factor and Minimum Spanning Tree are previously introduced. Area Fraction refers to the overall area fraction occupied by the Haversian canals in a specific region.

TABLE I Kruskall-Wallace nonparametric tests

Null (H_0)	The centers of all groups are equal		
Alternative (H_A)	At least one group center is shifted		
Test significance (α)	0.05		
Comparison	Test statistics (H)	p-value	Results
CA—by regions	123.88	<0.001	Reject null
SF—by regions	400.03	<0.001	Reject null
MST—by regions	18.19	0.003	Reject null

The three characteristic measurements of Haversian canals (CA, SF, and MST) are not normally distributed. The Canal Area (CA) and Shape Factor (SF) are generally right-skewed (skewness = 2.72, 0.54), while the MST branch distance is slightly left-skewed (skewness = −0.30). The datasets for CA, SF, and MST failed the Normality Test with their p-values less than 0.001. Therefore they were compared by the Kruskall-Wallace Nonparametric Tests. The region from which the canals were selected is the only factor to be compared in the nonparametric tests. The canals from the corresponding regions from all six sections were arranged in one group; thus we have 6 groups (1, 2L, 2R, 3L, 3R, and 4) representing the behavior from the 6 regions. This allows us to assess the difference among anterior (region 4), posterior (region 1), lateral (regions 2R & 3R), and medial (regions 2L & 3L) regions of the transverse sections. The results of the nonparametric tests are given in Table I. The large test statistics result in rejecting the null hypotheses for all the three microstructural parameters, CA, SF and MST, demonstrating that statistically significant differences exist among the various regions. These differences can be visualized from the side-by-side confidence intervals in Fig. 3a, b and c respectively. It is clear that regions 1 (posterior) and 4 (anterior) are not only different from the rest of the regions but also from each other. As seen from Fig. 3a and b, the Haversian canals in the posterior region are bigger (larger CA), have more non-circular cross-section (smaller SF), and are located at larger inter-canal distance (larger MST mean branch length) than those in the anterior regions. Furthermore, looking at the six sections together it appears that the area fraction occupied by the Haversian canals in the posterior region is the largest, and in the anterior region smallest (Table II). Overall, there is a negative correlation between the canal area and the shape factor. By matching the canal area with the shpae factor for every observation, the correlation coefficient is calculated to be −0.52, which indicates that the negative correlation is

TABLE II Average area fraction taken by the Haversian canals sorted by regions

	Regions					
Area fraction taken by Haversian canals (%)	1	2L	2R	3L	3R	4
	5.558	5.118	5.110	5.147	4.960	4.640

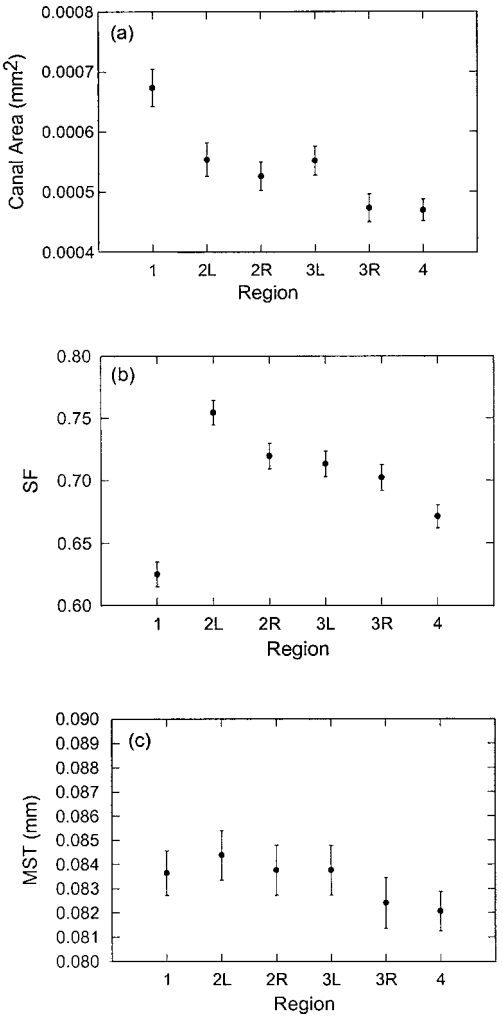

Figure 3 Confidence intervals for the (a) Canal Area, (b) Shape Factor, and (c) MST.

statistically significant and perceivable. This negative correlation implies that the larger the Haversian canals the more non-circular their shapes are.

3.2. Analyses of the lacunae-canal distances distribution

From the anterior and posterior regions, 15 osteons with circular-shape Haversian canals were randomly selected and classified into three canal sizes: *Small* ($<3.125\times10^{-4}$ mm^2), *Medium* ($3.125\times10^{-4}-5.000\times10^{-4}$ mm^2), and *Large* ($>5.000\times10^{-4}$ mm^2). For each osteon, the lacunae-canal distances were recorded. The dataset passes the Normality Test with a p-value 0.038 as the test significance (α) is set to be 0.01. In addition to normality, we assumed the homogeneity of variances and no subject effects so that the Analysis of Variance (ANOVA) can be applied to assess the differences.

2-Way ANOVA was performed and the test results are given in Table III. For the canal size factor, since the p-value is quite small (<0.0001), we can conclude that the canal size significantly affects the lacunae-canal distance. The box plot in Fig. 4 shows that the lacunae-canal distances increase with increasing canal sizes. For the region factor, although the test significance $\alpha = 0.05$ is larger than the p-value (0.013), it is, however,

TABLE III 2-Way ANOVA on the lacunae-canal distances in the regional comparison

Null (H_0)	All population means are equal
Alternative (H_A)	At least one mean differs from the rest
Test significance (α)	0.05
Test statistic (F)	11.33
p-value	<0.0001

Sources of variance	DF[a]	Sum of square	Mean square	F	p-value
Canal size	2	0.0062	0.0031	18.14	<0.0001
Region	1	0.0011	0.0011	6.26	0.0128
Interaction	2	0.0003	0.0001	0.83	0.4354

[a]DF: Degree of freedom.

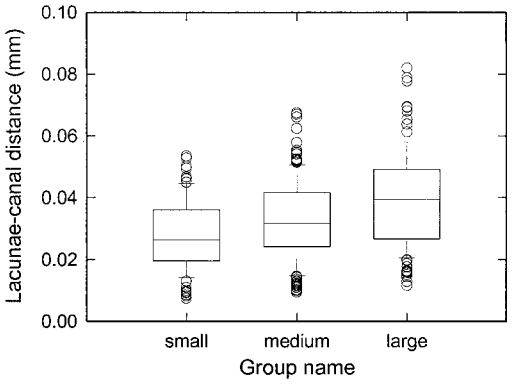

Figure 4 Side-by-side box plot of the lacunae-canal distances for the canal size factor in the regional comparison.

not safe to conclude its significance because the p-value is not very significantly less than α (a more stringent α, such as 0.01, could result in an opposite conclusion). Moreover, the "power" for the region factor was only 0.178. This implies that the probability of saying that region factor makes a difference when it really does is merely 17.8%.

The influence of region factor on the lacunae-canal distances cannot be revealed by a box plot because of the interference between the canal size factor and region factors; the canal area is on the average smaller in the anterior region and larger in the posterior region. Therefore, in order to visualize the effect of the region factor alone, we will make the size factor dimensionless by dividing the lacunae-canal distances with the effective radius of the Haversian canal, assuming the canal to be perfectly circular (SF = 1). Analysis of this ratio with 2-Way ANOVA is presented in Table IV. According to the p-values (region: 0.141; canal size: 0.013), we can conclude that, (i) the region factor has no effect on the ratio, and (ii) the canal size factor also has very little effect on the ratio. It is obvious from the box plot for the region factor, shown in Fig. 5, that the ratio of the lacunae-canal distances and the effective canal radius in the anterior and the posterior regions are nearly identical. This not only indicates that the region factor has no influence on the dimensionless ratio, but also suggests that the region does not affect the lacunae-canal distances. Therefore, we would not reject the null hypothesis for the region factor in the previous

TABLE IV 2-Way ANOVA on the dimensionless ratio in the regional comparison

Null (H_0)	All population means are equal
Alternative (H_A)	At least one mean differs from the rest
Test significance (α)	0.05
Test statistic (F)	2.95
p-value	0.0125

Source of variance	DF[a]	Sum of square	Mean square	F	p-value
Canal size	2	42.4860	21.2430	2.18	0.0129
Region	1	10.5104	10.5104	4.40	0.1409
Interaction	2	7.3110	3.655	0.76	0.4697

[a]DF: Degree of freedom.

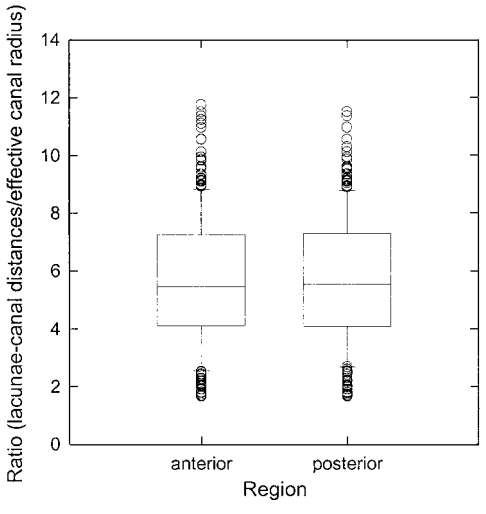

Figure 5 Side-by-side box plots of the dimensionless ratio for the region factor in the regional comparison.

2-Way ANOVA on the lacunae-canal distances. It is only the canal size differences in the anterior and posterior regions that affect the lacunae-canal distances; the two regions themselves do not affect the lacunae-canal distances.

Fig. 6 plots the distribution of the dimensionless ratio from all the 54 osteons examined in this study, irrespective of their regions. It shows that maximum number of lacunae is located at about 2.5 to 3 times the effective canal radius from the center of the Haversian canals. Only a few lacunae are located beyond the distance of 6 times the effective canal radius or within the distance of 2 times the effective canal radius. There are no discontinuous peaks in the distribution as would be expected if the surrounding lacunae were located at distances that are exact multiples of the effective radius of the Haversian canal.

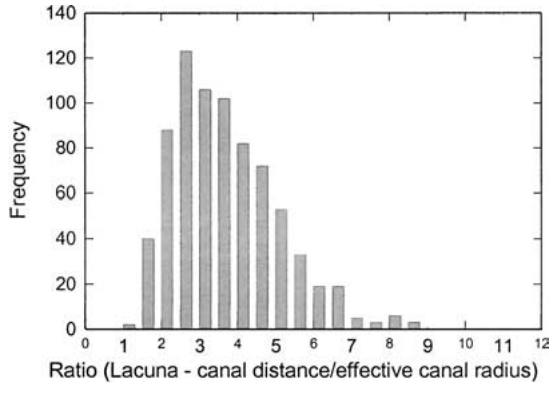

Figure 6 Distribution of the dimensionless ratio from 54 osteons.

3.3. Atomic force microscopy of features associated with the collagen fibers

Fig. 7 shows the microstructure in the posterior and the anterior regions as seen by atomic force microscopy. Collagen fibers are composed of numerous collagen-HA fibrils, the assembly of a lamella layer, causing the periodic banding of these fibers seen in the posterior and anterior regions. However, as shown in Fig. 7 the size distributions of these periodic banded features in the two regions show distinct differences. A single size distribution (29 ± 8 nm) is seen in the posterior region, but the anterior region shows portions with two distinct size distributions (67 ± 21 nm and 32 ± 9 nm). Further, it should be pointed out that in the posterior region there are occasionally large size features in the same region. However, in the anterior region the two size distributions are not found in the same region, but are located in regions that are separate from each other.

3.4. Three-dimensional reconstruction of the Haversian canals

Fig. 8 shows typical observations made from three-dimensional images of the Haversian canals from the anterior-medial region. Our reconstructed images resemble the three-dimensional osteons model proposed by Cohen and Harris [6] and demonstrate the complex patterns of organization dominated by branching. Haversian canals were seen to join (feature J), to branch, and to get enlarged (anastomosis, Feature E). Such an anastomosis may further develop into a large irregular space as the outcome of bone resorption, which Cohen and Harris [6] called the Haversian space. The wall-like empty space seen in feature HS of Fig. 8 may be part of the Haversian space. The Haversian canals are predominantly along the longitudinal direction. Some of them appear to be twisting gently as they course distally (features T in Fig. 8).

Blind osteons as defined by Cohen and Harris [6] are slightly tapered and end blindly without communicating with other systems. According to their observation, blind osteons are less commonly seen. In our study no blind osteons have been found.

4. Discussion

4.1. Haversian canals

There are various factors that affect bone growth, such as age, sex, disease states, exercise conditions, medicine treatments, etc. In this study, we did not compare the cortical bone from more than one designed group, but only focused on one tibia from a normal turkey; therefore, it is reasonable to expect that the different mechanical loading history upon each different region is the primary factor affecting the bone physiology. The

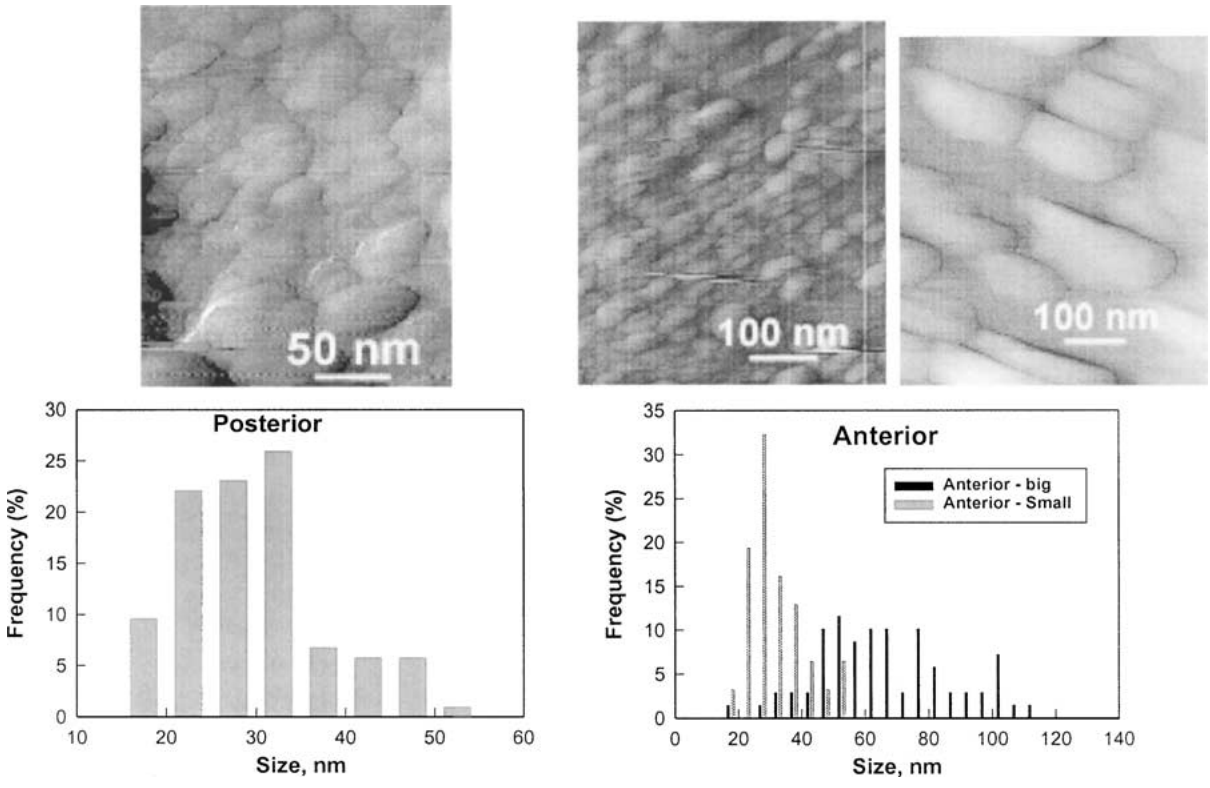

Figure 7 Collagen periodic banding observed in the AFM micrographs from the posterior (Bar = 50 nm) and anterior (Bar = 100 nm) for both micrographs) regions and their respective distributions.

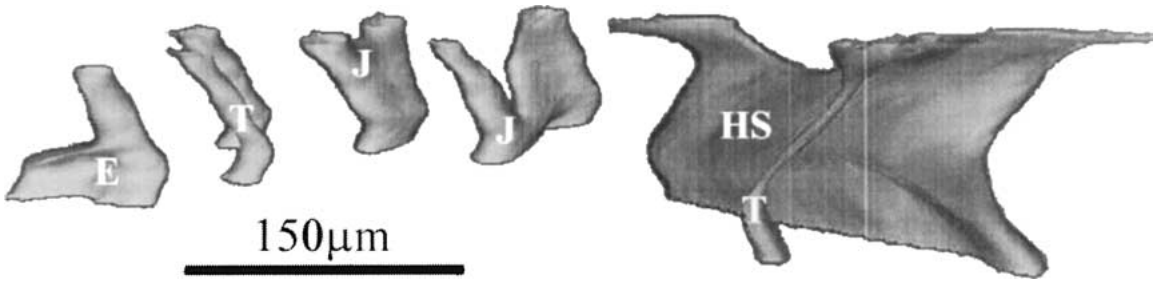

Figure 8 Three dimensional reconstructed images of the Haversian canals. Bar = 150 μm.

unusual differences that exist in the anterior and posterior regions may be best explained as a result of bending-induced relatively high tensile and compressive stresses, respectively, compared to the lateral and medial regions. Although the loading mode for a tibia is the combination of tension, compression, shear, torsion, and bending, bending is the most obvious and relevant mode that causes this uneven stress distribution—high tension in the anterior region and high compression in the posterior region [11, 12]. It is very likely that the growth and remodeling of the Haversian systems had been affected by this bending-induced uneven stress distribution in the cortical section of the long bone.

Our results show that the posterior region that is predominantly under compression has larger Haversian canals, that are more irregularly shaped, and are spaced at larger inter-canal distances as compared with the anterior region that is predominantly under tension (Fig. 3). Assuming that the cortical porosity is directly related to the area fraction of the Haversian canals we can also conclude that the posterior region is more porous than anterior region (Table II). It is interesting to note that engineering composites that are subject to tension are usually designed with closely spaced finer constituents and are less tolerant to porosity, as compared with those under compression that can tolerate higher levels of porosity. Our present observations confirm the long held belief that the nature responds to the prevailing stresses by adapting the Haversian system and bone microstructure accordingly.

Our study shows that osteons with larger Haversian canals tend to have more widely spread lacunae (Fig. 4). This trend can be expected as the development of the osteon and maturation of osteoblasts in lacunae closely relate to the transportation of nutrients and biochemical substances. The blood vessel within the Haversian canal is typically 15 μm in diameter according to the literature [13] and is capable of bringing nutrients within a limited range (about 150 μm) while Volkmann canals and canaliculi help the transport locally within the interstitial lamellae. Bigger Haversian canals have stronger mass transporting ability, allowing

wider osteons to be developed and also lead to longer lacuna-canal distances. We also observe that most of the lacunae are located at a distance of about 2.5 to 3 times the effective canal radius from the center of the Haversian canals, which probably is the required configuration for effective transport of the nutrients in the Haversian system. Only a few lacunae are located beyond the distance of 6 times the effective canal radius or within the distance of 2 times the effective canal radius.

In our three-dimensional reconstruction study we have ignored the lacunae and circumferential lamellae and focused only on the Haversian canal that represents the osteons axis. This approach adopted in the present investigation is similar to that of Heřt *et al*. [7] This gives the advantage of avoiding the complexity of the concentric circumferential lamellae while we are still able to recognize the orientation of the osteons. Unlike the previous three dimensional reconstruction studies that were concerned with millimeter to centimeter length scales and did not have well defined reference to accurately locate their transverse views [6–8] our observation is based on careful use of reference holes to position the serial sections. It looks at many Haversian canals but is limited to very short lengths, about 60 μm. It is interesting to note that over that short a distance, different canals with approximately 100 μm diameters show evidence of bifurcations, joining, gentle twisting and enlarged anastomosis. Even though the Haversian canals have a preferred alignment along the vertical axis they have a well-branched and complex morphology. There is a need to incorporate such morphology in modeling the mechanical behavior of bones, instead of the more common assumption that the bone-microstructure is similar to man-made composites with regular periodic arrangement of lamellae.

4.2. Atomic force microscopy of collagen fibers

Meager studies have been carried out on the bone using atomic force microscope and reported in the open literature. Nicolella *et al.* [4] have tried to characterize the damaged cortical bone of human femur after demineralization. They have reported the periodic banding of the collagen fibrils to be 70 nm. Sasaki *et al.* [5] have studied the structure of bovine femoral cortical bone at the collagen fibril-mineral level and reported that the periodic banding along the fiber was 67 ± 2 nm. Lees *et al.* [14] studied the demineralized dried Turkey leg tendon and reported the axial macroperiod of the banding as 73 nm. The bigger size (67 ± 21 nm) of the periodic features axial to the fibers observed in the present investigation is similar and in agreement with those reported earlier [3–5]. The minor variations in size of the periodic banding could be due to the species, location and method of preparation of the bone for observation etc. However, the smaller size at about 30 nm is certainly a different size distribution observed in the present investigation in both the anterior and the posterior regions. Earlier reports have not indicated two different size distributions. Although it is understood [11, 12] that the anterior and posterior regions are under tensile and compressive stresses respectively, it is difficult to attribute the observation of the bimodal distribution and the single size distribution in the respective regions to those stress states without further corroborating evidence. More thorough study and analysis are required to make any concrete conclusions.

5. Conclusions

Following conclusions can be made from our detailed statistical analysis of the microstructure of the cortical bone of Turkey tibia.

1. Haversian canals in the posterior region have larger cross-section area, more non-circular shape, and are spaced at longer inter-canal distance as compared with those in the anterior regions. The posterior region is more porous than anterior. The relatively high tension in the anterior region and high compression in the posterior region are believed to result in these distinct differences.

2. Osteons with larger Haversian canals tend to have more widely distributed lacunae, i.e., larger lacunae-canal distances. Majority of the lacunae are found at a distance of 2.5 to 3 times the Haversian canal radius. The ratio of the lacunae-canal distance and the effective radius of the canal is same in the anterior and posterior regions.

3. Three dimensional reconstruction of Haversian canals using accurate alignment of the transverse serial sections shows that even though the canals have a preferred alignment along the vertical axis they have a well branched and complex morphology containing bifurcations, gently twisted canals, and Haversian space. There was no evidence of blind canals. The longitudinal range of the reconstructed images is, however, limited to 60 μm.

4. Atomic force microscopy shows periodic banding of the collagen fibers at ultrastructural level. A bimodal banding distribution (67 ± 21 nm and 32 ± 9 nm) was found in the anterior region while only the finer banding distribution (29 ± 8 nm) was found in the posterior region.

Acknowledgments

Appreciation is expressed to Dr. R.B. Tripathi for helpful discussions.

References

1. R. AMPRINO and A. BAIRATI, *Z. Zelforsch.* **24** (1936) 439.
2. H. BROCKSTEDT, M. KASSEM, E. F. ERIKSEN, L. MOSEKILDE and F. MELSON, *Bone* **14** (1993) 681.
3. A. ARDIZZONI, *Bone* **28** (2001) 215.
4. D. P. NICOLELLA, D. E. MORAVITS, A. J. SILLER-JACKSON, R. J. RAILSBACK, S. F. TIMMONS, K. J. JEPSEN, D. T. DAVY and J. LANKFORD, *Amer. Soc. Mech. Engin., Bioengin. Div. BED* **42** (1999) 319.
5. N. SASAKI, A. TAGAMI, T. GOTO, M. TANIGUCHI, M. NAKATA and K. HIKICHI, *J. Mater. Sci.-Mater. Med.* **13**(3) (2002) 333.
6. J. COHEN and W. H. HARRIS, *J. Bone Joint Surg.* **40A** (1958) 419.

7. J. HEŘT, P. FIALA and M. PETRTÝL, *Bone* **15** (1994) 269.
8. S. D. STOUT, B. S. BRUNSDEN, C. F. HILDEBOLT, P. K. COMMEAN, K. E. SMITH and N. C. TAPPEN, *Calcif. Tissue Int.* **65** (1999) 280.
9. R. C. PRIM, *Bell Syst. Techn. J.* **36** (1957) 1389.
10. L. YU, G. L. DING, J. REYE, S. N. OJHA and S. N. TEWARI, *Metall. Mater. Trans.* A **30A** (1999) 2463.
11. B. DEMES, Y. X. QIN, J. T. STERN, JR., S. G. LARSON and C. T. RUBIN, *Amer. J. Phys. Anthrop.* **116** (2001) 257.
12. E. GAUTIER, S. M. PARREN and J. CORDEY, *J. Injury, Int. J. Care Injured* **31 S-C** (2000) 37.
13. R. B. MARTIN and D. B. BURR, "Skeletal Tissue Mechanics" (Springer-Verlag, NY, 1998).
14. S. LEES and S. PROSTAK, *Connect. Tissue Res.* **18** (1988) 41.

Received 11 November 2002
and accepted 18 August 2003